Contribution from the Department of Chemistry,
University of Minnesota, Minneapolis, Minnesota 55455

A Bis(μ-alkoxo)diiron Complex with Novel Terminally Ligated Carboxylates

Stéphane Ménage and Lawrence Que, Jr.*

Received April 3, 1990

The diferric complex $[Fe_2(DBE)_2(OBz)_2](ClO_4)_2$ (DBE = 2-[bis(2-benzimidazolylmethyl)amino]ethanol) was synthesized and characterized by NMR, IR, magnetic susceptibility, and X-ray crystallography methods. The title complex crystallizes in the space group $C2/c$ with $Z = 4$ ($a = 14.889$ (3), $b = 18.055$ (4), $c = 24.728$ (5) Å; $\beta = 101.67$ (2)°). The structure contains dimeric units where the two iron atoms are bridged by the oxygen atoms of the two DBE ligands, forming an $Fe_2(OR)_2$ core, and the two benzimidazoles on each tripod are coordinated trans to each other in planes perpendicular to the Fe_2O_2 core. The carboxylates are each ligated trans to one of the alkoxo bridges in an unusual coordination mode. The carbonyl oxygen is 2.89 (1) Å away from the iron center and appears to occupy a position in the coordination sphere. The iron(III) centers are antiferromagnetically coupled via the alkoxo bridges with $J = -20.5$ cm^{-1}. Chemical reduction of the complex leads to the formation of a mixed-valence species, with EPR features at $g = 1.94$ and 1.79. The relevance of this complex to the active sites of the iron–oxo proteins is discussed.

Oxo groups have been demonstrated to bridge the diferric centers in methemerythrin and ribonucleotide reductase and are characterized by short Fe–μ-oxo bond lengths, strong antiferromagnetic coupling ($-J > 100$ cm^{-1} for $\mathcal{H} = -2JS_1 \cdot S_2$), large Mössbauer quadrupole splittings, and enhanced Raman Fe–O–Fe vibrations.[1] Such a bridge appears unlikely for the diferric site in methane monooxygenase because of its apparently weaker antiferromagnetic coupling, the smaller Mössbauer quadrupole splittings, and the lack of significant visible absorption.[2,3] The oxygen bridge in this case is likely to be modified by protonation, alkylation, or acylation to conform with the spectroscopic and magnetic properties of the site.

Our interest in the active sites of iron-oxo proteins has led us to explore the iron chemistry of 2-[bis(2-benzimidazolylmethyl)amino]ethanol (DBE).[4] In an earlier study, Nishida et al.[5] reported a diferric complex of DBE with two benzoates and proposed a (μ-oxo)bis(μ-benzoato)diiron core structure capped by the nitrogen ligands of DBE with one of the dangling hydroxyethyl groups hydrogen bonded to the oxo bridge. Such a hydrogen bond would model the interaction of the bound hydroperoxide with the (μ-oxo)diiron(III) unit in oxyhemerythrin.[6] In reexamining this chemistry, we have crystallographically characterized a complex that has a bis(μ-alkoxo)diiron(III) core with the stoichiometry $[Fe_2(DBE)_2(OBz)_2]X_2$. In addition, this complex affords one of three known examples of terminal carboxylate coordination at a ferric center,[7,8] where the carboxylate does not constitute part of a polydentate ligand. We report the properties of this complex and the EPR signal of its mixed-valence derivative, the first from a bis(μ-alkoxo)diiron complex.

Table I. The Crystallographic Experiments and Computations[a] for **1**

formula	$C_{50}H_{48}Cl_2Fe_2N_{10}O_{15}$
fw	1211.59
temp, K	193
cryst syst	monoclinic
space group	$C2/c$
a, Å	14.889 (3)
b, Å	18.055 (4)
c, Å	24.728 (5)
β, deg	101.67 (2)
V, Å^3	6510 (4)
Z	4
D(calc), g cm^{-3}	1.236
cryst dimens, mm	0.150 × 0.2 × 0.25
radiation	Mo Kα (λ = 0.7107 Å)
monochromator	graphite
μ, cm^{-1}	4.69
scan type	ω
2θ max, deg	40.0
indices collcd	$h,k,\pm l$
no. of reflcns	3548 tot. 1194 used ($I > 3.00\sigma(I)$)
no. of least-squares params	196
data/params	6.09
R[b]	0.079
R_w[b]	0.09
GOF[b]	1.75
p[a]	0.05

[a] All calculations were performed by using the Texsan-Texray Structure Analysis Package, Molecular Structure Corp. (1985). The intensity data were processed as described in: *CAD 4 and SDP-PLUS User's Manual*; B. A. Frenz & Assoc.: College Station, TX, 1982. The net intensity was $I = [K(NPI)](C - 2B)$, where $K = 20.50$ (attenuator factor), NPI = ratio of fastest possible scan rate to scan rate for the measurement, C = total count, and B = total background count. The standard deviation in the net intensity is given by $[\sigma(I)]^2 = (k/NPI)^2[C + 4B + (pI)^2]$ where p is a factor used to downweight intense reflections. The observed structure factor amplitude F_o is given by $F_o = (I/Lp)^{1/2}$, where Lp = Lorentz and polarization factors. The $\sigma(I)$'s were converted to the estimated errors in the relative structure factors $\sigma(F_o)$ by $\sigma(F_o) = {}^1/_2[\sigma(I)/I]F_o$. [b] $R = (\sum||F_o| - |F_c||)/(\sum|F_o|)$; $R_w = \{(\sum w|F_o - F_c|^2)/(\sum w(F_o)^2)\}^{1/2}$; GOF = $\{(\sum w(|F_o| - |F_c|)^2)/(N_{data} - N_{params})\}^{1/2}$.

Experimental Section

Ligand. DBE was obtained from the reaction of *N*-(2-hydroxyethyl)iminodiacetic acid and *o*-phenylenediamine, both obtained from Aldrich, according to the procedure of Nishida.[9] ^{1}H NMR (δ, ppm, in DMSO/CD_3CN, 2:10): 7.52 (m, Bzim, 4 H), 7.16 (m, Bzim, 4 H), 3.9 (s, BzimCH_2, 4 H), 3.5 (m, CH_2–OH, 2 H), 2.7 (m, CH_2–CH_2N, 2 H).

(1) (a) Que, L., Jr.; True, A. E. *Prog. Inorg. Chem.*, in press. (b) Lippard, S. J. *Angew. Chem., Int. Ed. Engl.* **1988**, *27*, 344–361. (c) Sanders-Loehr, J. In *Iron Carriers and Iron Proteins*, Loehr, T. M., Ed.; VCH: New York, 1989; pp 375–466.
(2) Fox, B. G.; Surerus, K. K.; Münck, E.; Lispcomb, J. D. *J. Biol. Chem.* **1988**, *22*, 10553–10556.
(3) (a) Woodland, M. P.; Dalton, H. *J. Biol. Chem.* **1984**, *259*, 53–59. (b) Fox, B. G.; Froland, W. A.; Dege, J. E.; Lipscomb, J. D. *J. Biol. Chem.* **1989**, *264*, 10023–10033.
(4) Abbreviations used: DBE, 2-[bis(2-benzimidazolylmethyl)amino]-ethanol; OBz, benzoate; TTP, meso-tetra-*p*-tolylporphin; OAc, acetate; HPTB, *N,N,N',N'*-tetrakis(2-benzimidazolylmethyl)-2-hydroxy-1,3-diaminopropane; SALPAH, *N*-(hydroxypropyl)salicylideneamine; Fc, ferrocene; L, 1,4-piperazinediylbis(*N*-ethylenesalicylideneamine); phen, *o*-phenanthroline; N5, *N*-(2-hydroxyethyl)-*N,N',N'*-tris(2-benzimidazolylmethyl)-1,2-diaminoethane; *N*3, bis(2-benzimidazolylmethyl)amine; NTB, tris(2-benzimidazolylmethyl)amine; $HB(pz)_3$, hydrotris(pyrazolyl)borate; Me_3TACN, 1,4,7-trimethyl-1,4,7-triazacyclononane; tpbn, *N,N,N',N'*-tetrakis(2-pyridylmethyl)-1,4-diaminobutane; HXTA, *N,N'*-2-hydroxy-1,3-xylylenebis[*N*-(carboxymethyl)-glycine]; L', *N,N'*-ethylenebis((*o*-hydroxybenzyl)amine); acac, acetylacetonate anion; Chel, 4-hydroxo-2,6-pyridinedicarboxylate; Dipic = 2,6-pyridinedicarboxylate; $(CH_3)_2$N-pic, 4-dimethylamino-2,6-pyridinedicarboxylate; L'', trisalicylidenetriethylenetetramine.
(5) Nishida, Y.; Haga, S.; Tokii, T. *Chem. Lett.* **1989**, 169–172.
(6) Shiemke, A. K.; Loehr, T. M.; Sanders-Loehr, J. *J. Am. Chem. Soc.* **1986**, *108*, 2437–2443.
(7) Oumous, H.; Lecomte, C.; Protas, J.; Cocolios, P.; Guilard, R. *Polyhedron* **1984**, *6*, 651–659.
(8) Eremenko, I. L.; Pasynskii, A. A.; Orazsakhatov, B.; Ellert, O. G.; Novotortsev, V. M.; Kalinnikov, V. T.; Porai-Koshits, M. A.; Antsyshkina, A. S.; Dikareva, L. M.; Ostrikova, V. N.; Struchkov, Y. T.; Gerr, R. G. *Inorg. Chim. Acta* **1983**, *73*, 225–229.
(9) Nishida, Y.; Takahashi, K. *J. Chem. Soc., Dalton Trans.* **1988**, 691–699.

0020-1669/90/1329-4293$02.50/0

Table II. Selected Bond Lengths (Å) and Angles (deg) for $[Fe_2(DBE)_2(OBz)_2](ClO_4)_2$[a]

a. Bond Lengths			
Fe-O1	1.96 (1)	O1-C1	1.42 (2)
Fe-O1C	1.99 (1)	C1-C2	1.49 (3)
Fe-O1′	2.03 (1)	C2-N1	1.46 (2)
Fe-N1B	2.07 (2)	N1-C11A	1.51 (3)
Fe-N1A	2.09 (2)	N1-C11B	1.50 (3)
Fe-N1	2.35 (2)	N1A-C2A	1.32 (3)
O1C-C7C	1.30 (2)	C11A-C2A	1.45 (3)
O2C-C7C	1.22 (2)	C11B-C2B	1.49 (3)
C7C-C1C	1.52 (3)	N3A-C2A	1.35 (3)
		N1B-C2B	1.31 (3)
Fe-Fe	3.21 (1)	N3B-C2B	1.32 (3)
b. Bond Angles			
O1′-Fe-O1C	86.5 (5)	C1-O1-Fe	135 (1)
O1′-Fe-O1	72.5 (6)	C1-O1′-Fe	117 (1)
O1′-Fe-N1B	109.7 (7)	Fe-O1-Fe	107.4 (6)
O1′-Fe-N1A	104.1 (7)	Fe-N1-C2	106 (1)
O1C-Fe-O1	158.6 (5)	Fe-N1-C11A	107 (1)
O1C-Fe-N1B	92.7 (6)	Fe-N1-C11B	109 (1)
O1C-Fe-N1A	90.5 (7)	C2B-N1B-Fe	120 (2)
O1-Fe-N1B	90.6 (6)	C5B-N1B-Fe	137 (1)
O1-Fe-N1A	98.5 (7)	C7C-O1C-Fe	114 (1)
N1B-Fe-N1A	146.2 (7)	O2C-C7C-O1C	123 (2)
N1-Fe-O1	77.1 (7)	O2C-C7C-C1C	125 (2)
N1-Fe-O1′	149.1 (9)	O1C-C7C-C1C	112 (2)
N1-Fe-O1C	124.2 (7)	C2A-N1A-Fe	118 (2)
O1-C1-C2	110 (2)	C5A-N1A-Fe	135 (1)

[a] Estimated standard deviations in the least significant digits are given in parentheses.

$[Fe_2(DBE)_2(OBz)_2](ClO_4)_2 \cdot H_2O$. A mixture of 0.155 g (0.5 mmol) of DBE and 1 equiv of Et_3N (70 μL) was added to a methanolic solution (15 mL) of 0.187 g (0.5 mmol) of $Fe(ClO_4)_3 \cdot xH_2O$ and 0.061 g of benzoic acid (0.5 mmol). The initial yellow green solution turned to a bright orange solution and immediately yielded an orange microcrystalline powder. Yield: 56%. Anal. Calcd for $C_{50}H_{48}Cl_2Fe_2O_{15}N_{10}$: C, 49.56; H, 3.96; N, 11.56. Found: C, 49.32; H, 4.05; N, 11.32. UV-vis(CH_3CN): 310 (sh, ϵ = 18 000 M^{-1} cm^{-1}), 420 nm (sh). ^1H NMR (δ, ppm, in DMSO/CD_3CN, 2:10): 47.9, 36.1, 10.6, 7.9, 7.4, 5.9.

Crystallographic Studies. Due to the low solubility of $[Fe_2(DBE)_2(OBz)_2](ClO_4)_2$ in organic solvents, single crystals were obtained by slow diffusion of a methanolic solution of the iron salt via a frit into a solution of the carboxylate and ligand. After 1 week, orange plates suitable for X-ray structural analysis were obtained. Data were collected at the Crystallography Facility of the University of Minnesota Chemistry Department on an Enraf-Nonius CAD4 diffractometer at −80 °C on a crystal coated with a viscous high-molecular-weight hydrocarbon. Absorption corrections were made, and no signal decay was observed. The structure was solved by direct methods, and crystallographic and refinement data are summarized in Table I. Given the limited number of reflections, only the iron and chlorine atoms were refined anisotropically. Hydrogen atoms were included in the structure factor correlation in idealized positions (d(C-H) = 0.95 Å) and assigned isotropic thermal parameters which were 20% greater than the B_{eq} value of the atom to which they were bonded. The standard deviation of an observation of unit weight was 1.75. The weighting scheme was based on counting statistics and included a factor (p = 0.05) to downweight the intense reflections. The maximum and minimum peaks on the final difference Fourier map corresponded to 0.63 and −0.53 $e^-/Å^3$, respectively. Neutral-atom scattering factors were taken from Cromer and Waber.[10] All calculations were performed by using the TEXSAN crystallographic software package of the Molecular Structure Corp. Selected bond lengths and bond angles are listed in Table II, while the atomic coordinates, thermal factors, structure factors, and a complete listing of bond lengths and angles are available as supplementary material.

Physical Measurements. Magnetic susceptibility data were recorded over the temperature range 3.8–300 K at 10 kG with a SQUID susceptometer (Quantum Design, San Diego, CA) interfaced with an HP Vectra computer system. Samples (elemental analysis obtained) typically weighing 20–30 mg were used. The sample measurements were corrected for the diamagnetism of the sample bucket. The temperature dependence data for $[Fe_2(DBE)_2(OBz)_2](ClO_4)_2$ were analyzed by using the Heisenberg–Van Vleck spin Hamiltonian[11]

$$\mathcal{H} = -2JS_1 \cdot S_2 \quad (1)$$

where $S_1 = S_2 = 5/2$, by the use of the Van Vleck equation with the eigenvalues of the spin-coupling Hamiltonian. This gives rise to

$$\chi = \frac{Ng^2\mu_B^2(2e^{2x} + 10e^{6x} + 28e^{12x} + 60e^{20x} + 110e^{30x})}{kT(1 + 3e^{2x} + 5e^{6x} + 7e^{12x} + 9e^{20x} + 11e^{30x})} \quad (2)$$

where χ is the molar susceptibility and $x = J/kT$. The fit of the data to the Van Vleck equation was improved by the addition of a small amount of monomeric high-spin Fe(III) impurity. Thus eq 2 was modified in the following manner:

$$\chi = (1 - P)\chi' + 2P\chi_c + TIP \quad (3)$$

where χ is the total calculated susceptibility, χ' is the spin-coupled susceptibility calculated from eq 2, χ_c is the Curie law magnetic susceptibility for the monomeric Fe(III) impurity, P is the fraction of the paramagnetic impurity, and TIP is the temperature independent paramagnetism.

Infrared spectra were obtained on a Perkin Elmer FTIR 1600 series spectrometer. NMR spectra were run on an IBM AC300 spectrometer. EPR spectra were obtained at the X-band frequency with a Varian E-109 spectrometer equipped with an Oxford Instruments ESR-10 liquid-helium cryostat. Elemental analyses were performed at MHW Laboratories (Phoenix, AZ). UV-visible spectra were obtained on an HP 8541 diode array spectrophotometer. Electrochemical studies were performed with a BAS 100 electrochemical analyser under nitrogen at ambient temperature in a mixture of acetonitrile/DMSO (10:1) by using a three-electrode system consisting of a platinum working electrode, a platinum auxiliary electrode, and a $Ag/AgNO_3$ reference electrode separated from the bulk solution by a bridge of agar-agar in acetonitrile. The supporting electrolyte was 0.1 M tetrabutylammonium tetrafluoroborate, and the potentials were referenced with respect to the $Fc^{+/0}$ couple (+85 mV vs $Ag/AgNO_3$).

Results and Discussion

Previously, we have investigated the iron coordination chemistry of the ligand *N,N,N′,N′*-tetrakis(2-benzimidazolylmethyl)-2-hydroxy-1,3-diaminopropane (HPTB) to model the active sites of iron–oxo proteins. Two ferric complexes were synthesized, $[Fe_4O_2(HPTB)_2(OBz)_2](ClO_4)_2(OTs)_2$ and $[Fe_2(HPTB)(OBz)_2](ClO_4)_3$.[12] In this paper, we focus on the iron chemistry of the tripodal ligand DBE, which essentially consists of half the dinucleating ligand HPTB. Contrary to the proposal of Nishida et al.,[5] the DBE complex has been characterized by X-ray diffraction to have a bis(μ-alkoxo)diiron core with the formulation $[Fe_2(DBE)_2(OBz)_2](ClO_4)_2$.

Crystal Structure of $[Fe_2(DBE)_2(OBz)_2](ClO_4)_2 \cdot H_2O$. The complex crystallizes in the space group $C2/c$. An ORTEP plot of the centrosymmetric cation is shown in Figure 1, and the principal structural parameters of the cation are listed in Table II. The structure shows a dimeric unit where the two iron atoms are bridged by the oxygen atoms of the two ligands, forming a $Fe_2(OR)_2$ core. The center of symmetry lies in the center of this core. The Fe–O–Fe angle is 107.4 (6)° comparable to those found in $[Fe(SALPA)(SALPAH)]_2$ (110.6 (9) and 108.2 (9)°),[13] $[FeL(OCH_3)_2Cl_2]$ (103 (1)°),[14a] $[FeL(OC_2H_5)_2Cl_2]$ (104.3 (1)°),[14b] and $[FeCl_3(OC_2H_5)]_2]^{2-}$ (107.0 (3)°).[15] The Fe–Fe separation is 3.21 (1) Å, identical with that for $[Fe(SALPA)(SALPAH)]_2$[11] but larger than those found by Chiari[14] in his compounds (3.106 (7) and 3.144 (1) Å for the methoxide and ethoxide, respectively).

Each iron atom has an N_3O_3 donor set in a distorted octahedron with the amine N1 and benzoate O1C trans to the μ-alkoxo bridges. The two benzimidazole nitrogen atoms are trans to each other and lie on an axis perpendicular to the Fe_2O_2 plane. This arrangement allows for ring-stacking interactions to occur between benzimidazoles on different DBE ligands, which may contribute to the stability of this structure.[16] The average Fe–N(benz-

(10) Cromer, D. T.; Waber, J. T. *International Tables for X-Ray Crystallography* The Kynoch Press: Birmingham, England, 1974; Vol. IV, Table 2.2 A.

(11) O'Connor, C. J. *Prog. Inorg. Chem.* **1979**, *29*, 204–283.
(12) Chen, Q.; Lynch, J. B.; Gomez-Romero, P.; Ben-Hussein, A.; Jameson, G. B.; O'Connor, C. J.; Que, L., Jr. *Inorg. Chem.* **1988**, *27*, 2673–2681.
(13) Bertrand, J. A.; Eller, P. G. *Inorg. Chem.* **1974**, *13*, 927–934.
(14) (a) Chiari, B.; Piovesana, O.; Tarantelli, T.; Zanazzi, P. F. *Inorg. Chem.* **1982**, *21*, 1396–1402. (b) Chiari, B.; Piovesana, O.; Tarantelli, T.; Zanazzi, P. F. *Inorg. Chem.* **1984**, *23*, 3398–3404.
(15) Walker, J. D.; Poli, R. *Inorg. Chem.* **1990**, *29*, 756–761.

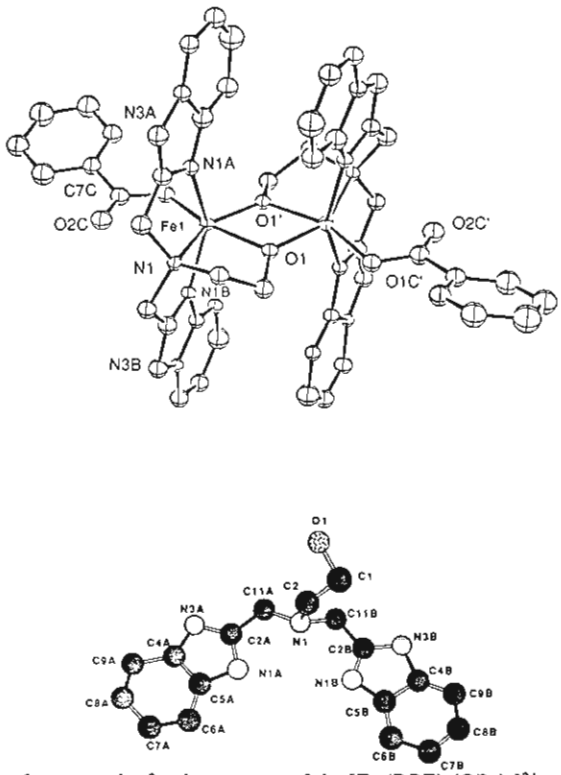

Figure 1. ORTEP plot for the structure of the $[Fe_2(DBE)_2(OBz)_2]^{2+}$ cation (top) and a scheme showing the atom-labeling scheme of the DBE ligand (bottom).

imidazole) distance is 2.08 (2) Å and is in the same range as those found in $[(N5)FeOFeCl_3]^+$ (2.086 (5) Å)[17] and $[(N3)Fe(OBz)]_2O(ClO_4)_2$ (2.108 (7) Å),[18] and the Fe-N(imidazole) bonds in $[Fe_3O(TIEO)_2(OBz)_2Cl_3]$ (2.146 (6) Å).[19] The Fe–O(alkoxo) bonds are inequivalent at 1.96 (1) and 2.03 (1) Å. Similar asymmetry is found for the cores of other bis(μ-alkoxo) complexes such as $[Fe(SALPA)(SALPAH)]_2$ (Fe–O = 1.92 (2) and 2.00 (2) Å)[13] and $[FeCl_3(OC_2H_5)]_2]^{2-}$ (1.940 (6) and 2.011 (6) Å).[16] The Fe–O(carboxylate) distance is 1.99 (1) Å, close to those found in $[Fe_4O_2(HPTB)_2(OBz)_2](ClO_4)_2(OTs)_2$ (2.029 (2) and 2.014 (2) Å).[10]

This structure has two interesting features. The Fe–N(amine) distance, 2.35 (2) Å, is rather long particularly when compared to those of related tripodal ligand complexes like $[Fe_2O(TPA)_2(OBz)](ClO_4)_3$ (2.190 (6) and 2.218 (6) Å).[20] However, such long Fe–N(amine) bonds seem to be characteristic of complexes of polydentate ligands containing benzimidazole such as $[Fe_4O_2(HPTB)_2(OBz)_2](ClO_4)_2(OTs)_2$ (2.306 (2) Å),[10] $[(N5)FeOFeCl_3]^+$ (2.357 (5) Å),[17] $[(N3)Fe(OBz)]_2O(ClO_4)_2$ (2.284 (6) Å),[18] and $[(NTB)_2Fe_2O(OBz)](ClO_4)_3$ (2.402 (6) and 2.338 (6) Å).[21] It seems likely that the elongation is a result of constraints imposed by the incorporation of the imidazole (vis-ã-vis pyridine) ring into a five-membered chelate ring structure.

The other interesting feature is the observed benzoate coordination mode. Though carboxylates are known to act as bidentate bridging ligands in diferric complexes,[22] there are only two other examples thus far of a structurally characterized iron(III) complex where a carboxylate that is not part of a polydentate ligand binds in a monodentate mode[7,8] and no examples of a chelated carboxylate. In the DBE complex, the benzoate is best characterized as primarily monodentate but having a weak secondary interaction via the carbonyl oxygen (Figure 2). The Fe–O1C bond length is not unusual for an iron(III) carboxylate interaction (1.99 (1) Å), but the O1C–Fe–N1 angle of 124.2 (7)° is distorted from its octahedral optimum. The benzoate is coordinated via O1C using its more basic syn lone pair, while the other benzoate oxygen atom O2C lies between O1 and N1 in the plane defined by O1, O1′, N1, and O1C. The Fe–O1C–C7C angle of 114 (1)° is sufficiently acute to afford the O2C oxygen an Fe–O distance of 2.89 (1) Å. Though this is a weak interaction by any criterion, this oxygen atom appears to occupy a position in the iron coordination sphere, resulting in the expansion of the O1C–Fe–N1 angle.[23]

Many of the structural features of $[Fe_2(DBE)_2(OBz)_2](ClO_4)_2$ can also be found in $[Fe(DBE)_2(NO_3)_2](NO_3)_2$.[24] The complex

Table III. Comparison of Magnetic Properties of Diferric Complexes with Fe_2O_2 Cores

	J, cm^{-1}	ref
bis(μ-alkoxo)		
$[Fe(SALPA)(SALPAH)]_2$	−17	13
$[FeL(OCH_3)_2Cl_2]$	−16.3	14a
$[FeL(OC_2H_5)_2Cl_2]$	−15.3	14b
$[FeL(acac)_2(OC_2H_5)_2]$	−11.0	14b
$[Cl_3Fe(OC_2H_5)_2FeCl_3]^{2-}$	−26.4	15
$[Fe_2(DBE)_2(OBz)_2]^{2+}$	−20.5	this work
bis(μ-hydroxo)		
$[Fe(Dipic)(H_2O)(OH)]_2$	−11.4	25
$[Fe(Chel)(H_2O)(OH)]_2{\cdot}4H_2O$	−7.3	25
$[Fe((CH_3)_2N\text{-pic})(H_2O)(OH)]_2$	−11.7	26
$[FeL'OH]_2{\cdot}2H_2O{\cdot}2py$	−10.4	27
(μ-phenoxo)(μ-alkoxo or hydroxo)		
$[Fe_2(5\text{-MeHXTA})OH(H_2O)]$	−12	28
$[FeL''(OH)Cl_2]$	−7.4	29
$[FeL''(OCH_3)Cl_2]$	−8.0	30
bis(μ-phenoxo)		
$[Fe(salen)Cl]_2$	−7.5	31

Table IV. Comparison of Carboxylate Stretching Modes

	ν_{as}, cm^{-1}	ν_s, cm^{-1}	$\Delta\nu$, cm^{-1}	ref
bidentate, bridging	1580	1410–1440	140–170	34
bidentate, nonbridging	1510–1550	1450–1470	40–80	34
monodentate	1600–1725	1267–1380	220–460	34
$[Fe_2(DBE)_2(OBz)_2]^{2+}$	1554	1379	175	this work
$[Fe_2(HPTB)(OBz)_2]^{3+}$	1556	1358	198	12
$[Fe_4O_2(HPTB)(OBz)_2]^{4+}$	1544	1400	144	12
Fe(TTP)OAc	1668	1259	409	7
$Cp_3Cr_3FeS_4(O_2C\text{-}t\text{-}Bu)$	1635	1320	315	8

(16) Ring stacking interactions can also be found in $[Fe_2O(phen)_4(H_2O)_2](ClO_4)_4$: Plowman, J. E.; Loehr, T. M.; Schauer, C. K.; Anderson, O. P. *Inorg. Chem.* **1984**, *23*, 3553–3559.

(17) Gomez-Romero, P.; Witten, E. H.; Reiff, W. M.; Backes, G.; Sanders-Loehr, J.; Jameson, G. B. *J. Am. Chem. Soc.* **1989**, *111*, 9039–9047.

(18) Gomez-Romero, P.; Casan-Pastor, N.; Ben-Hussein, A.; Jameson, G. B. *J. Am. Chem. Soc.* **1988**, *110*, 1988–1990.

(19) Gorun, S. M.; Papaefthymiou, G. C.; Frankel, R. B.; Lippard, S. J. *J. Am. Chem. Soc.* **1987**, *109*, 4244–4255.

(20) (a) Yan, S.; Cox, D. D.; Pearce, L. L.; Juarez-Garcia, C.; Que, L., Jr.; Zhang, J. H.; O'Connor, C. J. *Inorg. Chem.* **1989**, *28*, 2507–2509. (b) Norman, R. E.; Yan, S.; Que, L., Jr.; Backes, G.; Ling, J.; Sanders-Loehr, J.; Zhang, J. H.; O'Connor, C. J. *J. Am. Chem. Soc.* **1990**, *112*, 1554–1562.

(21) Menage, S.; Que, L., Jr. Unpublished results.

(22) Examples include $[Fe_2O(TPA)_2(OBz)](ClO_4)_3$,[19] $[Fe_2O(Me_3TACN)_2(OAc)_2](ClO_4)_2$,[22a] $[Fe_2O(HB(pz)_3)_2(OAc)_2]$,[22b] and $[Fe_2O(tpbn)(OAc)_2]_2(NO_3)_4$.[22c] (a) Hartman, J. R.; Rardin, R. L.; Chaudhuri, P.; Pohl, K.; Wieghardt, K.; Nuber, B.; Weiss, J.; Papaefthymiou, G. C.; Frankel, R. B.; Lippard, S. J. *J. Am. Chem. Soc.* **1987**, *109*, 7387–7396. (b) Armstrong, W. H.; Lippard, S. J. *J. Am. Chem. Soc.* **1983**, *105*, 4837–4838. (c) Toftlund, H.; Murray, K. S.; Zwack, P. R.; Taylor, L. F.; Anderson, O. P. *J. Chem. Soc., Chem. Commun.* **1986**, 191–193.

(23) Tolman et al. recently reported a diferrous complex where the carbonyl oxygen of a O,O-bridging formate occupies one vertex of an "octahedral" Fe(II) center at a distance of 2.79 Å, thus affording a carboxylate ligand that is similarly asymmetrically chelated: Tolman, W. B.; Bino, A.; Lippard, S. J. *J. Am. Chem. Soc.* **1989**, *111*, 8522–8523.

(24) Nishida, Y.; Shimo, H.; Takahashi, K.; Kida, S. *Mem. Fac. Sci., Kyushu Univ., Ser. C*, **1984**, *14*, 301–306.

(25) Thich, J. A.; Ou, C. C.; Powers, D.; Vassiliou, B.; Mastropaolo, D.; Potenza, J. A.; Schugar, H. J. *J. Am. Chem. Soc.* **1976**, *98*, 1425–1432.

(26) Ou, C. C.; Lalancette, R. A.; Potenza, J. A.; Schugar, H. J. *J. Am. Chem. Soc.* **1978**, *100*, 2053–2057.

(27) Borer, L.; Thalken, L.; Cecarrelli, C.; Glick, M.; Zhang, J. H.; Reiff, W. M. *Inorg. Chem.* **1983**, *22*, 1719–1724.

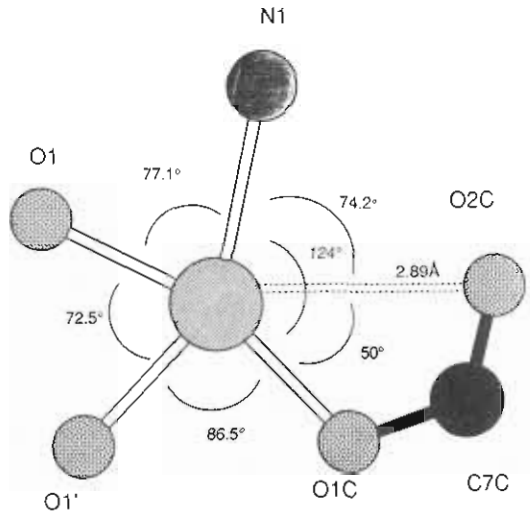

Figure 2. Detail of the iron coordination sphere for the $[Fe_2(DBE)_2(OBz)_2]^{2+}$ cation.

has a $Fe_2(OR)_2$ core, elongated Fe–N(amine) bonds (2.311 (8) Å), and enlarged N(amine)–Fe–O(nitrate) angles to allow asymmetric chelation of the nitrates (2.067 (10) and 2.682 (10) Å). The weaker nitrate ligand gives rise to shorter Fe–OR and Fe–N bonds relative to those in the benzoate complex and a tighter Fe_2O_2 core structure (r_{Fe-Fe} = 3.176 (3) Å). There are thus two examples of DBE complexes where XO_2-type ligands can chelate asymmetrically to the Fe(III) centers; we conjecture that this is due to the enhanced Lewis acidity of the Fe(III) centers resulting in part from the particularly weak Fe–N(amine) bond.

Other examples of structurally characterized Fe(III) complexes with a monodentate carboxylate are [FeTTP(OAc)][7] and $[Cp_3Cr_3FeS_4(O_2C\text{-}t\text{-}Bu)]$.[8] In both cases, the acetate coordinates to the iron via its syn lone pair but appears not to have the secondary carbonyl interaction suggested by the structure of the DBE complex. [FeTTP(OAc)] has the typical square-pyramidal coordination sphere of a 5-coordinate metalloporphyrin complex. The Fe–O(carbonyl) distance is 3.130 (4) Å, the Fe–O–C angle is 130.0 (2)°, and the O–Fe–N(TTP) angles are ca. 107.0 (2)°, as expected for a 5-coordinate porphyrin complex with the metal center 0.485 (2) Å above the porphyrin plane. The iron appears tetrahedrally coordinated in $[Cp_3Cr_3FeS_4(O_2C\text{-}t\text{-}Bu)]$ with O–Fe–S angles of 115 (1)° and S–Fe–S angles of 104 (1)°.[8] Though the Fe–O(carbonyl) distance is 2.94 (1) Å, the iron coordination sphere is not particularly distorted in the vicinity of the carbonyl oxygen, as found in the DBE complexes. Furthermore, the COO vibrations in the IR spectra of these two complexes indicate monodentate carboxylate coordination, in contrast to what is observed with the DBE complex (Table IV, vide infra). We speculate that the lack of a secondary carboxylate interaction in the latter complexes is a result of the weaker Lewis acidity of these iron centers.

Physical Properties of $[Fe_2(DBE)_2(OBz)_2](ClO_4)_2\cdot H_2O$. Magnetic susceptibility measurements on a powder sample of $[Fe_2(DBE)_2(OBz)_2](ClO_4)_2$ between 300 and 3.8 K show that the two metal ions are antiferromagnetically coupled. Very good agreement between theory and experimental data was obtained by using the following parameters: g = 2.05, J = −20.5 cm^{-1}, % imp = 0.92, and TIP = 4.3 × 10^{-5} (Figure 3).

The J value obtained for the DBE complex, which is in agreement with that reported by Nishida,[5] lies on the higher end of the range of values found for complexes with Fe_2O_2 cores. Table

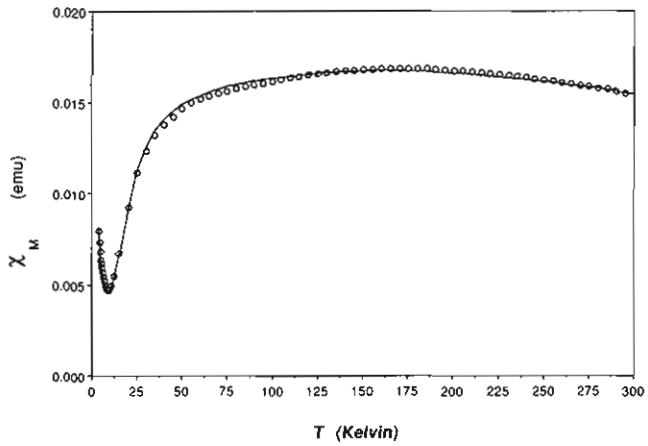

Figure 3. Plot of χ_M vs T for solid $[Fe_2(DBE)_2(OBz)_2](ClO_4)_2$. The dashed line represents the best least-squares fit of eq 3 (see text) to the experimental susceptibility data (g = 2.05; J = −20.5 cm^{-1}; % imp = 0.92; TIP = 4.3 × 10^{-5}).

III shows a representative list for comparison. In general, the presence of a phenoxo bridge or bis(μ-hydroxo) bridges in these complexes gives rise to $-J$ values near 10 cm^{-1}, while complexes with bis(μ-alkoxo) bridges in general afford $-J$ values nearer 20 cm^{-1}. For comparison, tribridged diferric complexes with J values in this general range include $[Fe_2(HBpz_3)_2(OH)(OAc)_2]ClO_4$[32] with a ($\mu$-hydroxo)bis($\mu$-acetato)diferric core (−17 cm^{-1}) and $Me_4N[Fe_2(HXTA)(OAc)_2]$[33] with a (μ-phenoxo)bis(μ-acetato)-diferric core (−10 cm^{-1}). The rationale for these trends is not yet determined.

The ^{1}H NMR spectrum of the DBE complex shows paramagnetically shifted features out to 50 ppm. The shifts observed are commensurate with the extent of antiferromagnetic coupling determined from the magnetic susceptibility experiments. A broad peak at 47 ppm disappears upon addition of D_2O to the NMR solution and is therefore assigned to the benzimidazole N–H protons. The sharper feature at 34 ppm is not solvent exchangeable and is assigned to C–7H (β to benzimidazole NH) by analogy to the Fe_2HPTB complexes.[12] Similarly, sharp features at 10.6 and 5.9 ppm correspond to the meta and para protons of the coordinated benzoates, respectively. Other peaks in the NMR spectrum are difficult to assign unequivocally and will require atom-substituted derivatives.

The infrared spectrum of the complex shows two strong features at ca. 1379 and 1554 cm^{-1}, assigned to ν_s(COO) and ν_{as}(COO), respectively (Table IV). The ν_s(COO) feature fits with the values found for metal complexes with monodentate carboxylates (range 1267–1380 cm^{-1});[34] however ν_{as}(COO) has a value closer to those associated with nonbridging bidentate modes (1510–1550 cm^{-1}) and distinct from those associated with monodentate coordination (1600–1725 cm^{-1}). Nakamoto has shown that it is possible to distinguish between the coordination mode of a carboxylate according to the difference between the two stretching energies, $\Delta\nu$ ($\nu_{as} - \nu_s$).[34] For a bidentate bridging carboxylate, $\Delta\nu$ is between 140 and 170 cm^{-1}; for a bidentate nonbridging mode, $\Delta\nu$ is 40–80 cm^{-1} and is more than 220 cm^{-1} for monodentate coordination. The COO vibrations of Fe(TPP)OAc and $Cp_3Cr_3FeS_4(O_2C\text{-}t\text{-}Bu)$ are consistent with the monodentate acetate coordination mode ($\Delta\nu$ = 409 and 315 cm^{-1}, respectively). In the DBE case, $\Delta\nu$ is 175 cm^{-1}, an ambiguous value based on Nakamoto's correlations. However, the deviation from the standard values for carboxylate coordination may be rationalized by the presence of the added weak interaction between the metal and the carbonyl oxygen from the carboxylate, which makes the benzoate ligand in this complex

(28) Murch, B. P.; Bradley, F. C.; Boyle, P. D.; Papaefthymiou, V.; Que, L., Jr. *J. Am. Chem. Soc.* **1987**, *109*, 7993–8003.
(29) Chiari, B.; Piovesana, O.; Tarantelli, T.; Zanazzi, P. F. *Inorg. Chem.* **1983**, *22*, 2781–2784.
(30) Chiari, B.; Piovesana, O.; Tarantelli, T.; Zanazzi, P. F. *Inorg. Chem.* **1982**, *21*, 2444–2448.
(31) Reiff, W. M.; Long, G. J.; Baker, W. A. *J. Am. Chem. Soc.* **1968**, *90*, 6347–6351.
(32) Armstrong, W. H.; Lippard, S. J. *J. Am. Chem. Soc.* **1984**, *106*, 4632–4633.
(33) (a) Murch, B. P.; Bradley, F. C.; Que, L., Jr. *J. Am. Chem. Soc.* **1986**, *108*, 5027–5028. (b) Murch, B. P. Ph.D. Thesis, Cornell University 1987.
(34) Nakamoto, K. *Infrared and Raman Spectra of Inorganic and Coordination Compounds*, 4th ed.; Wiley: New York, 1986; pp 231–233.

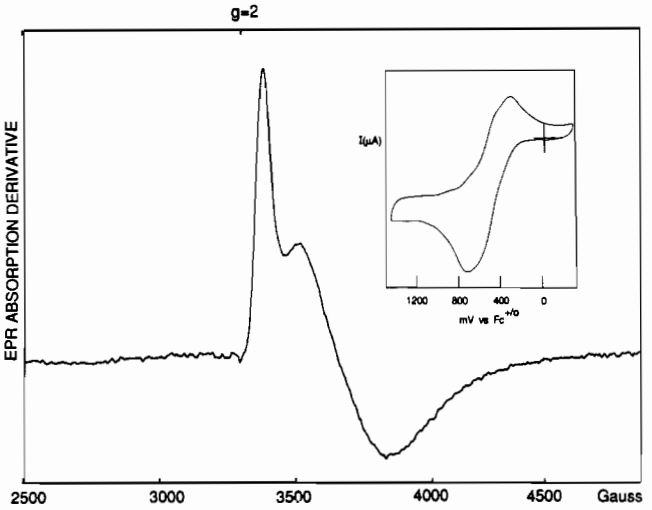

Figure 4. EPR spectrum of the mixed-valence diiron(II,III) complex at 4.5 K in acetonitrile with 0.2 mW microwave power, modulation amplitude of 1 G, modulation frequency of 100 kHz, and time constant of 0.25 s. Inset: the cyclic voltammogram of $[Fe_2(DBE)_2(OBz)_2](ClO_4)_2$ in CH_3CN/DMSO (10:1).

more than monodentate in character.

Comparison with $[Fe_2(HPTB)(OBz)_2]X_3$. Many of the properties discussed above for the DBE complex are shared by $[Fe_2(HPTB)(OBz)_2](ClO_4)_3$, which has not been structurally characterized.[12] The latter complex has a $-J$ value of 26 cm^{-1}, NMR shifts for the benzimidazole and benzoate protons are very similar to the DBE complex, and IR $\nu_s(COO)$ and $\nu_{as}(COO)$ features are at 1358 and 1556 cm^{-1}, respectively ($\Delta\nu$ = 198 cm^{-1}). These similarities and the IR data, in particular, suggest that the benzoates in the latter complex are coordinated in a manner similar to that for the benzoates in the DBE complex and not the asymmetric bridging mode we preferred in our earlier paper.[12] The implications of these similarities to the structure of $[Fe_2(HPTB)(OBz)_2](ClO_4)_3$ are currently being investigated.

Mixed-Valence Species. Cyclic voltammetric results for $[Fe_2(DBE)_2(OBz)_2]^{2+}$ (Figure 4 inset) show a reduction at −745 mV vs $Fc^{+/0}$ and reoxidation at −355 mV. We attribute the reduction wave to the reduction of the $Fe^{III}Fe^{III}$ complex to its $Fe^{III}Fe^{II}$ form. The electrochemical process was found to be kinetically dependent because of variations in the shape of the voltammogram at different scan speeds (50–300 mV/s), probably due to the decomposition of the mixed-valence complex. Controlled-potential coulommetry on the complex shows that the mixed-valence complex is unstable at room temperature (n_{e^-} = 1.3), with the solution changing from yellow to colorless via an intermediate orange species.

Due to the apparent instability of $[Fe_2(DBE)_2(OBz)_2]^+$ at room temperature under the coulometric conditions, the diferric compound was chemically reduced. Treating $[Fe_2(DBE)_2(OBz)_2](ClO_4)_2$ with 1 equiv of cobaltocene in a mixture of acetonitrile/DMSO at ambient temperature followed by rapid cooling to 77 K yields an orange-red solution that is EPR active. The complex exhibits EPR signals at g = 1.94 and 1.79 (Figure 4) with $g_{av} \sim 1.84$. That all g values are less than 2 is indicative of an antiferromagnetically coupled $Fe^{III}Fe^{II}$ species with an $S = {}^1/_2$ ground state.[35] Such features are analogous to those found for the mixed-valence forms of the iron–oxo proteins such as purple acid phosphatase (1.95, 1.72, 1.56),[36] azidosemimethemerythrin (1.95, 1.72, 1.69),[37] and methane monooxygenase (1.93, 1.87).[2]

Double integration of the EPR signal with copper(II) sulfate as a standard indicates that the signal corresponds to 50% of the intensity expected from the concentration of the starting diferric complex, further emphasizing the instability of the mixed-valence species. Attempts to estimate the value of J for the mixed-valence complex using the temperature dependence of the power saturation of its EPR signal[38] have been unsuccessful due to difficulties in saturating the EPR signal. It is thus likely that $-J$ is small (<10 cm^{-1}).

Implications for the Iron–Oxo Proteins. We have characterized a bis(μ-alkoxo)diiron(III) complex with an Fe–Fe separation of 3.216 Å and a J of −20.5 cm^{-1}, and its mixed-valence form exhibits EPR signals with g values <2. These properties suggest that such a core must be considered when analyzing the data for the iron–oxo proteins that do not have an oxo bridge, e.g., methane monooxygenase (MMO). MMO lacks any significant visible absorption that can be attributed to a bent Fe–O–Fe unit[3] and exhibits significant population of a paramagnetic excited state (assumed to be S = 1) at 20 K in its Mössbauer spectrum,[2] which implies a $-J$ value of no greater than 20 cm^{-1}. This value is presently consistent with complexes having $Fe_2(\mu\text{-}OR)(\mu\text{-}RCO_2)_2$ or $Fe_2(\mu\text{-}OR)_2$ cores. The absence of significant visible absorption in MMO eliminates tyrosine as a potential ligand and suggests that the OR bridge(s) may be either hydroxide or alkoxide. The observation of a 3.4-Å Fe–Fe separation in the EXAFS spectrum of the mixed-valence form of MMO,[39] similar to that observed for semimethemerythrin azide,[40] is consistent with an $Fe_2(\mu\text{-}OR)(\mu\text{-}RCO_2)_2$ core structure.[32,33,41] This distance would also be consistent with an $Fe_2(OR)_2$ core, since it may be expected to expand upon one-electron reduction; unfortunately, the instability of the one-electron-reduced DBE complex prevents its further structural characterization. The DBE complex with its novel carboxylate coordination mode also has relevance with respect to the recently solved crystal structure of the B2 subunit of the ribonucleotide reductase from *Escherichia coli*.[42] There are in the protein four carboxylates ligated to the diiron unit, each in a distinct coordination mode. One carboxylate is coordinated in a syn monodentate mode; whether a secondary carbonyl interaction may be present will depend on further refinement of the crystallographic data.

Acknowledgment. This work was supported by the National Institutes of Health (Grant GM-38767). We are grateful to Professor J. D. Britton for his expertise in the X-ray diffraction experiments.

Supplementary Material Available: ORTEP figure with complete atom-labeling scheme and tables of atomic coordinates, thermal parameters, and complete bond lengths and bond angles for $[Fe_2(DBE)_2(OBz)_2](ClO_4)_2$ (20 pages); a table of structure factors (9 pages). Ordering information is given on any current masthead page.

(35) Palmer, G.; Brintzinger, H.; Estabrook, R. W.; Sands, R. H. In *Magnetic Resonance in Biological Systems*; Ehrenberg, A., Malmström, B., Vänngard, T., Eds.; Pergamon Press: New York, 1967; pp 159–171.
(36) Day, E. P.; David, S. S.; Peterson, J.; Dunham, W. R.; Bonvoisin, J. J.; Sands, R. H.; Que, L., Jr. *J. Biol. Chem.* **1988**, *263*, 15561–15567.
(37) Muhoberac, B. B.; Wharton, D. C.; Babcock, L. M.; Harrington, P. C.; Wilkins, R. G. *Biochim. Biophys. Acta* **1980**, *626*, 337–345.
(38) Rutter, R.; Hager, L. P.; Dhonau, H.; Hendrich, M.; Valentine, M.; Debrunner, P. *Biochemistry* **1984**, *23*, 6809–6816.
(39) Ericson, A.; Hedman, B.; Hogdson, K. O.; Green, J.; Dalton, H.; Bentsen, J. G.; Beer, R. H.; Lippard, S. J. *J. Am. Chem. Soc.* **1988**, *110*, 2330–2332.
(40) Scarrow, R. C.; Maroney, M. J.; Palmer, S. M.; Que, L., Jr.; Roe, A. L.; Salowe, S. P.; Stubbe, J. *J. Am. Chem. Soc.* **1987**, *109*, 7857–7864.
(41) (a) Borovik, A. S.; Papaefthymiou, V.; Taylor, L. F.; Anderson, O. P.; Que, L., Jr. *J. Am. Chem. Soc.* **1989**, *111*, 6183–6195. (b) Mashuta, M. S.; Webb, R. J.; Oberhausen, K. J.; Richardson, J. F.; Buchanan, R. M.; Hendrickson, D. N. *J. Am. Chem. Soc.* **1989**, *111*, 2745–2746.
(42) Nordlund, P.; Sjöberg, B.-M.; Eklund, H. *Nature* **1990**, *395*, 593–598.